CMNS Research Progressing in Kobe University
-Deuterium Permeation and Absorption–

A. Kitamura[1]*, T. Yamaguchi[1], T. Nohmi[1], Y. Sasaki[1], Y. Miyashi[1], A. Taniike[1], Y. Furuyama[1],

and A.Takahashi[2]

[1]Division of Marine Engineering, Graduate School of Maritime Sciences, Kobe University

[2]Professor Emeritus, Osaka University

*kitamura@maritime.kobe-u.ac.jp

Experimental studies on condensed matter nuclear science (CMNS) ongoing in Kobe University are reviewed. One is the subject of nuclear transmutation during forced permeation of deuterium (D) through multi-layered films of CaO/X/Pd, with X being an element to be transmuted, which is described in detail in the present paper.

The second subject is to confirm heat and ^{4}He generation by D absorption in nano-sized Pd powders reported by Arata and Zhang, and to investigate the underlying physics. We have installed a twin system to perform calorimetry during D_2 or H_2 absorption by micronized powders of Si, Pd, Pd-black, and Pd-Zr oxide compounds. The research is performed as a joint research program with Technova Inc., and is described in detail in the separate two papers presented by the joint group in the present proceedings.

Keywords: Nuclear transmutation, Condensed matter nuclear science, Permeation, Accelerator analysis, Sputtering

1. Introduction

It has been claimed that forced permeation of deuterium (D) through X-deposited (Pd/CaO)/Pd samples induced nuclear transmutation from the element X to Y, where (X, Y) being (^{133}Cs, ^{141}Pr), (^{88}Sr, ^{96}Mo), (^{138}Ba, ^{150}Sm) and (^{137}Ba, ^{149}Sm) [1,2]. In our previous work [3] to replicate the phenomena, we used XPS to characterize the CaO/Sr/Pd sample. The XPS method has a high sensitivity of detection limit, 7×10^{12} atoms/cm^2, but it is applicable only to the near-surface (< 3 nm) region, and is necessarily destructive when measurement of the depth distribution over tens of nm is required.

The basic configuration of the samples used in the present work is vacuum/(CaO/Sr/Pd)$_n$/CaO/Sr/Pd/(D$_2$) with exception of some runs with no CaO layer or with additional Pd layer on the top, where n = 9 or 0. In the samples used in refs. [1,2], the nuclei to be transmuted are located on the sample surface, and exposed to D_2 gas atmosphere. In most of the present work, however, they are embedded in the sample between the CaO layer and the Pd layer/bulk, and exposed to D permeating through the sample. Accordingly, we use PIXE to measure nondestructively the time-dependent concentration of the elements in the sample *in situ* and simultaneously, at the cost of increasing the sensitivity limit to 1×10^{14} atoms/cm^2.

In addition to the modified version of the sample exposure system [3,4] with reversed flow direction installed at a beam line of a tandem electrostatic accelerator 5SDH-2, a stand-alone D permeation system [5] is used to examine the phenomenon by *in-situ* or *ex-situ* PIXE/ERD analysis, respectively.

2. Experimental apparatus and procedure

The major system is an *in-situ* system shown in Fig. 1. The film was mounted on a vacuum flange with O-ring seal, and the rear surface was exposed to D_2 gas for 7 - 48 days. The sample area effective for D permeation was 3.7 cm², and the D_2 gas pressure was maintained at 0.04 - 0.1 MPa by occasionally replenishing the reservoir. The D flow rate through the complex sample kept at 70°C was 0.01 – 0.15 sccm, which was calculated from the pressure change. We performed *in situ* analyses for characterization of the sample before, during and after D permeation, namely, 3-MeV proton PIXE for elemental analysis, 2.5-MeV ³He NRA or 4-MeV ⁴He ERDA for D distribution analysis. The ⁴He ERDA method has a spatial resolution of about 100 nm. For monitoring the incident particle fluence, RBS was applied simultaneously.

The other system, the *ex-situ* system shown in Fig. 2, is a D-absorption apparatus arranged independently of the accelerator analysis system. In the analysis, we intended to make a large incident angle (85°) measurement to increase PIXE sensitivity. First, we made PIXE analysis, before mounting the sample on a vacuum flange to expose the rear surface to D_2 gas at a

pressure of 0.1 MPa. After finishing D permeation the PIXE analysis was made again, while NRA and ERDA for D distribution analysis were skipped in the *ex-situ* runs.

Fabrication procedure for the CaO/Sr/Pd sample is as follows. A 0.1-mm-thick Pd plate was annealed for 3 to 10 hours at 570 - 1170 K, and then immersed in aqua regia/H_2O or aqua regia/D_2O for 100 seconds. Sr atoms were deposited on one side of the Pd bulk surface using electrochemical deposition, by carefully placing the Pd bulk plate on the surface of the 10-mM $Sr(NO_3)_2/D_2O$ solution. Finally, a CaO layer with a thickness of 2 - 8 nm was deposited on the Sr/Pd samples. For samples containing thin layers of Pd such as Pd/CaO/Sr/Pd and $(CaO/Sr/Pd)_9/CaO/Sr/Pd$, the Pd thin layers with thickness of 54 nm or 18 nm were deposited also by RF sputtering.

3. Results of permeation runs

As typical examples, the PIXE spectra observed in the Run 15 for the sample $(V)/Pd/CaO/Sr/Pd/(D_2)$ are shown in Fig. 3(a). A pair of K_α-K_β X-ray peaks are clearly found for Sr. However, those for Mo are rather difficult to identify, although an analysis software
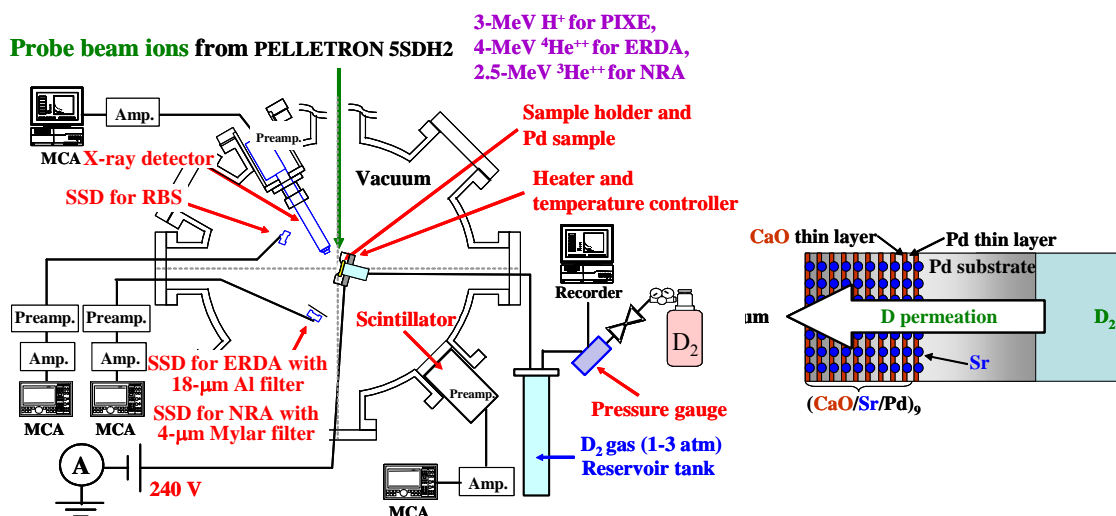

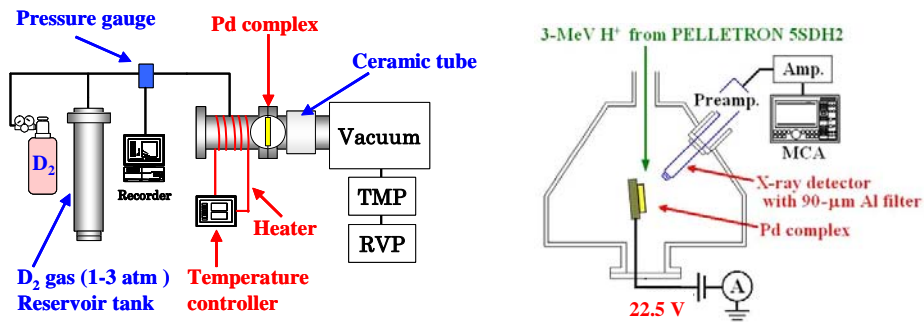Fig.1. A schematic of the *in situ* experimental setup (left), and an example of the sample configuration (right).

Fig. 2. A schematic of the gas permeation system (left) and the *ex situ* sample characterization system (right).

GUPIXWIN [6] can calculate the areal density of Mo, A_{Mo}, with little certainty based on the measured spectra. The areal densities of Sr and Mo, A_{Sr} and A_{Mo}, respectively, given by GUPIXWIN are shown in Fig. 3(b) as a function of the time-integrated flow rate, or the permeation fluence of D, F_D. A slight increase $(0.6 \times 10^{15}$ cm$^{-2})$ in A_{Mo} accompanied by a more pronounced decrease $(3.1 \times 10^{15}$ cm$^{-2})$ in A_{Sr} is observed after the 490-hour permeation run.

Distribution of D at 350 h $(F_D = 7.8 \times 10^{22}$ cm$^{-2})$ measured by ^{4}He-ERDA is shown in Fig. 3(c). Although the D density of about 2×10^{22} cm^{-3} (PdD$_{0.29}$) near the surface is relatively low, it increases toward the depth to the saturation value of 5.8×10^{22} cm^{-3} (PdD$_{0.85}$) at about 0.5 μm. This implies that release of D$_2$ molecules following recombination of atomic D at the vacuum/Pd interface is sufficiently fast, and the D flow is diffusion-limited in the near-surface region incorporating the CaO/Sr/Pd interface. On the surface,

H concentration amounts 5 – 10 % of the total hydrogen isotope density, which is probably due to ion-beam-induced hydrocarbon deposition from gas phase contaminants. Since the distribution FWHM is almost the same as the spatial resolution of 100 nm, the H atoms are expected to be localized in the uppermost layer with little mixing with bulk D atoms.

Table I summarizes the results of all runs including those for samples with W additive described later in section 5. For the *in-situ* samples, *i.e.*, run #6 through #15, PIXE and ERDA measurements were performed several times during a run. The values of A_{Sr} and A_{Mo} listed in the table are those obtained in the first and the last measurements, while those of the D fluence and the composition D/Pd are at the end of the absorption run. For the *ex-situ* samples, *i.e.*, run #B1 through #B4, the PIXE measurements were done for 8 - 26 different points on each sample, and the averaged values are given in Table I.
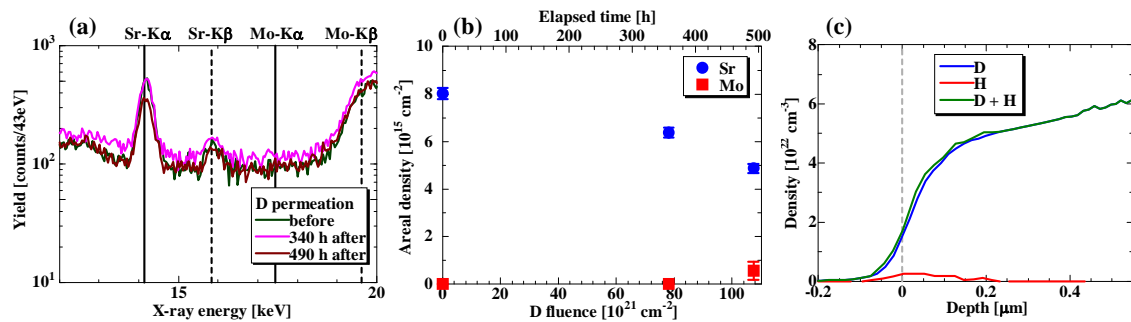

Fig. 3. (a) PIXE spectra, (b) temporal variation of the areal densities of Sr and Mo expressed as a function of D fluence (time-integrated flow rate), and (c) density profiles of hydrogen isotopes measured at 350 h in the Run 15.

Table I. Summary of permeation runs for samples with Sr or W additive.

Run #	Sample configuration (V)=vacuum, M=CaO/Sr/Pd	D flow rate (sccm)	D flux (sccm/cm^2)	Time (h)	D fluence (10^{22}cm^{-2})	D/Pd	Areal density (10^{15}cm^{-2}) before - after	
							Sr / W	Mo / Pt
6	(V)/CaO/Sr/Pd/(D$_2$)	0.42	0.114	1170	21.1	0.56	2.6 - 2.6	5.0 - 4.7
7	(V)/CaO/Sr/Pd/(D$_2$)	0.062	0.017	610	1.64	0.4	21.2 - 15.3	1.3 - 1.1
8	(V)/CaO/Sr/Pd/(D$_2$)	0.08	0.022	470	1.63	0.81	4.6 - 3.8	1.2 - 1.0
9	(V)/CaO/Sr/Pd/(D$_2$)	0.049	0.013	2320	4.39	0.59	2.5 - 2.5	0 - 1.2
10	(V)/M^9/CaO/Sr/Pd/(D$_2$)	0.47	0.127	620	12.6	0.86	49.5 - 52.0	0.2 - 0.4
11	(V)/Pd/M^9/CaO/Sr/Pd/(D$_2$)	0.03	0.008	970	1.33	0.02	24.1 - 21.3	0 - 0.8
12	(V)/Sr/Pd/CaO/Pd/(D$_2$)	0.64	0.173	440	12.4	--	3.5 - 2.2	0 - 0
13	(V)/Sr/Pd/CaO/Pd/(D$_2$)	0.35	0.095	660	10.1	0.07	5.0 - 4.4	0 - 0.5
14	(V)/Pd/CaO/Sr/Pd/(D$_2$)	0.026	0.007	470	0.51	--	4.4 - 4.2	0 - 0.8
15	(V)/Pd/CaO/Sr/Pd/(D$_2$)	0.5	0.135	490	10.7	0.78	8.0 - 4.9	0 - 0.6
B1	(V)/CaO/Sr/Pd/(D$_2$)	0.05	0.021	930	4.44	--	5.2 - 0.7	0.1 - 0.1
B2	(V)/Pd/CaO/Sr/Pd/(D$_2$)	0.07	0.029	810	5.4	--	8.1 - 1.5	0.3 - 0.4
B3	(D$_2$)/Sr/Pd/CaO/Pd/(V)	0.09	0.024	570	2.33	--	3.4 - 1.4	0.3 - 0.2
B4	(D$_2$)/Sr/Pd/CaO/Pd/(V)	0.34	0.092	590	8.77	--	18.8 - 7.8	0.3 - 0.4
16	(V)/Pd/CaO/W/Pd/(D$_2$)	1.31	0.354	170	9.87	0.17	0.16 - 0.04	2.1 - 1.2
17	(V)/Pd/CaO/W/Pd/(D$_2$)	0.26	1.44	170	39.6	--	0.82 - 0.82	0.35 - 0.34

In every run we were unable to find any element having the atomic number between 38 (Mo) and 46 (Pd) in the PIXE spectra. In some runs marginal increase in A_{Mo} was observed in exchange for decrease in A_{Sr}, but with little quantitative consistency; an increase in A_{Mo} was too little to compensate the decrease in A_{Sr}. In other runs we sometimes have decreasing areal densities of both Sr and Mo.

Moreover, identification of Mo peak by GUPIXWIN was not definite in most cases. We need Mo atoms with areal density larger than 3×10^{15} cm^{-2} to make a clear identification by PIXE analysis.

However, it is interesting to note that A_{Sr} decreased with increasing D fluence in most runs, which is clearly seen in Fig. 4(a), where A_{Sr} normalized to the initial value in each run are traced. On the other hand, in about half of the runs A_{Mo} is increasing, which is traced in Fig. 4(b).

A possible reason for the decrease might be sputtering by 3-MeV protons used as the probe beam for PIXE analysis and/or 4-MeV ^{4}He for ERDA. A simulation program ACAT [7] has been employed to estimate the sputtering yield for a Sr target to show that

contribution of sputtering to the decrease would be 2 orders of magnitude smaller than the decrease observed. However, the sputtering yield for deposited atoms weakly bonded to the bulk atoms should be much larger than the bulk atoms.

The sputtering yields calculated for 1-keV proton incidence on various target materials are plotted in Fig.
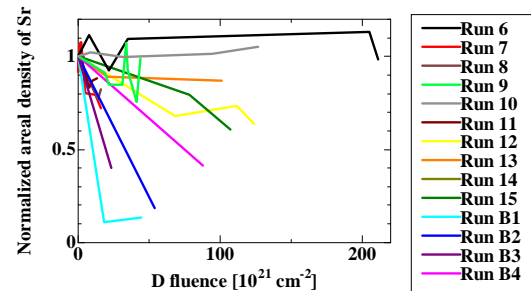

Fig. 4(a). Normalized areal density of Sr plotted against fluence (integrated flow rate) of deuterium.
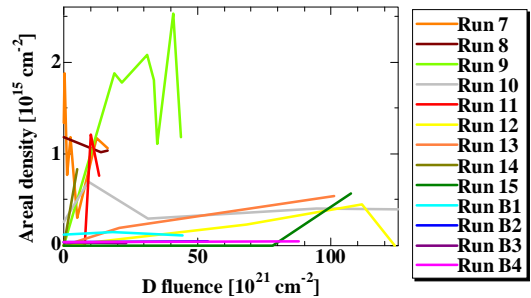

Fig. 4(b). Areal density of Mo plotted against fluence (integrated flow rate) of deuterium.
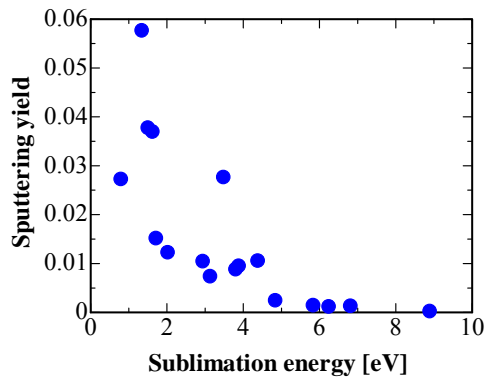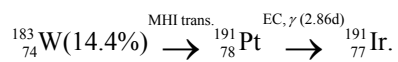
Fig. 5. Calculated sputtering yield by 1-keV protons plotted as a function of sublimation energy for various materials.

Fig. 6. Gamma ray spectra measured for a Pd/CaO/W/Pd sample after D permeation up to a fluence of 3.96×10^{23} cm^{-2}.

5 as a function of the sublimation energy of the material. It is implied that the sputtering yield for atoms such as those adsorbed, which have bonding energies of the order of 0.1 eV, can be orders of magnitude greater than the bulk atoms. This could account for the decrease in A_{Sr}. If this is the case, the measured values of A_{Mo} are also suffering from the sputtering loss, which could result in the apparently smaller "transmutation" yield.

5. Possible transmutation to radioisotope

If the transmutation product is a radioisotope, the detection will be extremely easier. The detection limit would be as low as 10^5 atoms/cm^2. If we assume the regularity of transformation that the atomic number and the mass number increase by 4 and 8, respectively, we can expect production of the following radioisotope emitting 0.538-MeV γ rays;

$$^{183}_{74}W(14.4\%) \xrightarrow{\text{MHI trans.}} {}^{191}_{78}Pt \xrightarrow{\text{EC, } \gamma \text{ (2.86d)}} {}^{191}_{77}Ir.$$

For this purpose, we prepared samples with a structure (V)/Pd/CaO/W/Pd/(D$_2$). The thickness of the first Pd layer and the second CaO layer were 38 nm and 2 nm, respectively. The tungsten atoms were introduced into the samples by implantation with 380-keV W^{++} ions accelerated by the tandem Pelletron, and were
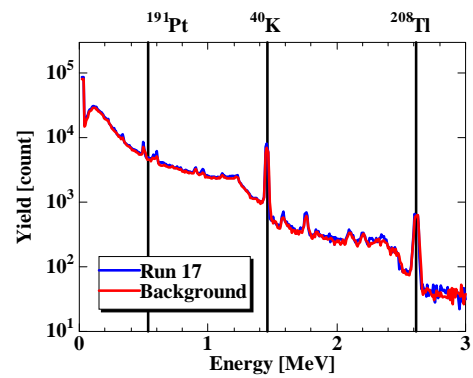
expected to distribute at a depth of 40 nm with a range straggling of 16 nm.

Before and after D permeation, PIXE measurements were performed to reveal existence of W and Pt as shown in Table I. The latter is one of impurity elements contained in the virgin Pd samples with no radioactive isotope of ^{191}Pt. The tendency of decreasing areal densities of both W additive and impurity Pt was again confirmed as seen in Table I.

Gamma ray measurements were performed with an NaI(Tl) scintillation probe during permeation, and an HPGe detector after finishing the permeation. An example of the output spectrum from the latter detector is shown in Fig. 6. Unfortunately, we were unable to find the 0.538-MeV γ ray peak in the spectra.

6. Conclusions for transmutation works

Employing both *in situ* and *ex situ* accelerator analyses, we have tried to replicate the nuclear transmutation of Sr to Mo under deuterium permeation through a variety of multilayered CaO/Sr/Pd samples. Apparently positive results were obtained in 8 runs out of 14, although the identification of Mo peaks in the PIXE analysis was not definite. It has been implied that sputtering loss of the atoms could be responsible for the observed tendency that areal density of Sr decreases in

most cases, while increase in that of Mo is modest.

In addition to the accelerator analyses, γ-ray detection was tried for samples implanted with W atoms in expectation of transmutation from [183]W to radioactive [191]Pt, however without positive result yet.

We have at least three problems to be solved in future research; to improve the sample uniformity, to increase the D permeation rate, and to increase the amount of the additive atoms to be transmuted.

7. Deuterium Absorption to Pd Powders

Results on the second subject obtained by the cooperative work with Technova Inc. [8,9] is briefly summarized here.

To confirm heat and [4]He generation by deuterium (D) absorption in nano-sized Pd powders reported by Arata and Zhang, and to investigate the underlying physics, we have installed a twin system of double structured vessels to perform flow calorimetry during D_2 or H_2 absorption by a variety of micronized Pd samples. We can perform D_2 and H_2 absorption runs for two samples at the same time under the same environmental condition.

Characteristics of deuterium/hydrogen absorption and accompanying heat generation have been compared for three kinds of Pd powders; commercially available 0.1-$\mu m \phi$ Pd powder, commercially available Pd-black, and nano-sized powder of mixed Pd and Zr oxides fabricated by Santoku Cooperation, Kobe, Japan. It has been found that the D(H)/Pd ratio and absorption energy is an increasing function of fineness of the sample surface.

The Pd·Zr mixed oxides have revealed their interesting and exciting characteristics:

1) D-gas charge in the 1st phase (zero pressure interval) gave 35 % excess heat compared to H-gas charge. In the 2nd phase of pressure rise up to the final 1 MPa, significant excess heat of about 2 kJ/g-Pd for D-gas charge was observed, while essentially zero output energy was observed for H-gas charge.

2) D(H)/Pd loading ratio reached very large values of 1.1 at the end of the 1st phase.

3) Released energy per D- or H-atom in the 1st phase was 2.2 - 2.5 eV/D or 1.3 - 2.1 eV/H, which are anomalously large compared with known values of 0.5 eV and 0.2 eV per D- or H-atom respectively for surface adsorption and lattice absorption of hydrogen atoms into bulk Pd metal.

4) No increase of neutron counts was seen, nor increase of gamma-ray counts.

References

[1] Y. Iwamura, M. Sakano and T. Itoh: Jpn. J. Appl. Phys. 41 (2002) 4642-4650.

[2] Y. Iwamura *et al.*: Proc. ICCF12, 2005, Yokohama, Japan, (World Scientific Publishing Co. Pte. Ltd, 2006) 178-187.

[3] A. Kitamura, R. Nishio, H. Iwai, R. Satoh, A. Taniike and Y. Furuyama: Proc. ICCF12, 2005, Yokohama, Japan, (World Scientific Publishing Co. Pte. Ltd, 2006) 272-277.

[4] T. Yamaguchi, T. Nohmi, H. Iwai, A. Taniike, Y. Furuyama, and A. Kitamura: Proc. 8th Meeting of Japan CF Research Society, Nov. 29-30, 2007, Doshisha Univ. (JCF Research Soc., 2008) 15-19.

[5] T. Yamaguchi, Y. Sasaki, T. Nohmi, A. Taniike, Y. Furuyama, A. Kitamura, and A. Takahashi: http://www.ler-canr.org; to be published in Proc. 14th Int. Conf. Condensed Matter Nuclear Science (ICCF14), Aug. 10-15, 2008, Washington DC.

[6] J. L. Campbell: http://pixe.physics.uoguelph.ca/gupix/main/.

[7] Y. Yamamura and Y. Mizuno : IPPJ-AM-40 (Institute of Plasma Physics, Nagoya Univ., 1985).

[8] Y. Sasaki, A. Kitamura, T. Nohmi, Y. Miyoshi, A. Taniike, A. Takahashi, R. Seto, and Y. Fujita: Deuterium Gas Charging Experiments with Pd Powders for Excess Heat Evolution, (I) Results of absorption experiments using Pd powders, this Proceedings.

[9] A.Takahashi, A. Kitamura, T. Nohmi, Y. Sasaki, Y. Miyoshi, A. Taniike, R. Seto, and Y. Fujita: Deuterium Gas Charging Experiments with Pd Powders for Excess Heat Evolution, (II) Discussions on Experimental Results and Underlying Physics, this Proceedings.